

Design and Synthesis of Fluorinated Amphiphile as ^{19}F MRI/Fluorescence Dual-Imaging Agent by Tuning the Self-Assembly

Shaowei Bo,^{†,‡,§} Cong Song,[‡] Yu Li,[‡] Weijiang Yu,[‡] Shizhen Chen,^{||} Xin Zhou,^{||} Zhigang Yang,[‡] Xing Zheng,^{*,†,§} and Zhong-Xing Jiang^{*,‡,§}

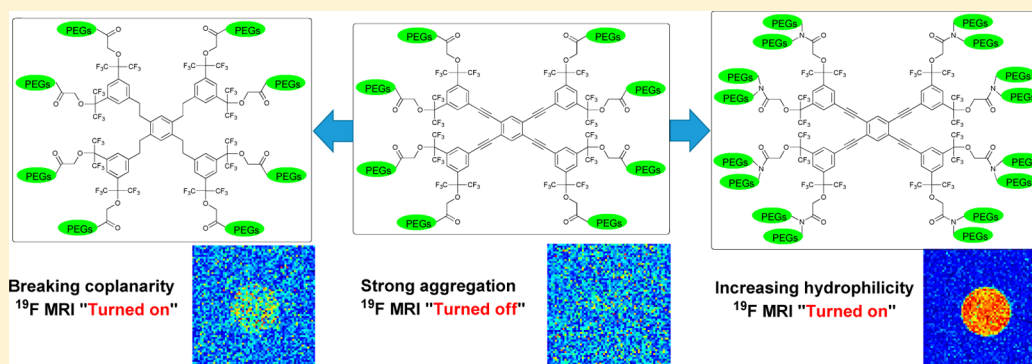
[†]Institute of Pharmacy & Pharmacology, University of South China, Hengyang 421001, China

[‡]Key Laboratory of Combinatorial Biosynthesis and Drug Discovery (Wuhan University), Ministry of Education and Wuhan University School of Pharmaceutical Sciences, Wuhan 430071, China

^{||}Key Laboratory of Magnetic Resonance in Biological Systems, State Key Laboratory for Magnetic Resonance and Atomic and Molecular Physics, National Center for Magnetic Resonance in Wuhan, Wuhan Institute of Physics and Mathematics, Chinese Academy of Sciences, Wuhan 430071, China

[§]Hunan Province Cooperative Innovation Center for Molecular Target New Drug Study, Hengyang 421001, China

S Supporting Information



ABSTRACT: Both ^{19}F MRI and optical imaging are powerful noninvasive molecular imaging modalities in biomedical applications. To integrate these two complementary imaging modalities, the design and synthesis of a novel ^{19}F MRI/fluorescence dual-modal imaging agent is reported herein. Through Sonogashira coupling reaction between the fluorinated phenylacetylene and 1,2,4,5-tetraiodobenzene, a fluorophore with 48 symmetrical fluorines at its periphery was constructed with high efficacy. High aqueous solubility was achieved by PEGylation of the fluorophore with monodisperse PEGs. However, an unexpected self-assembly of the PEGylated amphiphilic fluorophore in water “turned off” the ^{19}F NMR signal. However, hydrogenation of the triple bonds or introduction of branched monodisperse PEGs was able to efficiently tune the self-assembly, resulting in the “turning on” of the ^{19}F NMR signal. One of these amphiphiles combines the advantages of label-free fluorescence, high ^{19}F MRI sensitivity, biocompatibility, and excellent aqueous solubility. The results demonstrate the great potential of such amphiphiles for real-time ^{19}F MRI and fluorescence dual-modality imaging.

INTRODUCTION

Integration of multiple imaging modalities is an efficient way to achieve precise and fast imaging of targets of interest in biomedical diagnosis. In recent years, many multimodal imaging agents/probes have been developed and found to exhibit superb imaging capabilities.¹ Among the various combinations of imaging modalities, the combination of magnetic resonance imaging (MRI) and fluorescence imaging is highly advantageous. On one hand, MRI generates detailed anatomic images of opaque objects without tissue depth limits and ionizing radiation. However, it suffers the drawbacks of low sensitivity and long imaging times. On the other hand, fluorescence imaging provides real-time images with high sensitivity, but it can hardly image internal organs. Thus,

integration of these two complementary imaging modalities into a novel MRI/fluorescence dual-imaging agent is the cornerstone for downstream biomedical applications.

Among the stable nuclei used in MRI, ^1H has the highest sensitivity, and therefore, ^1H MRI is the technique used most frequently in clinic imaging diagnosis. Unfortunately, the strong background signals in ^1H MRI result in low contrast ratios. ^{19}F MRI has an advantage over ^1H MRI owing to the lack of endogenous background signals, which gives ^{19}F MRI a high contrast-to-noise ratio and specificity for the detection of exogenous ^{19}F contrast agents. Moreover, the 100% natural

Received: April 12, 2015

Published: May 27, 2015



Figure 1. Target ^{19}F MRI and fluorescence dual-modal imaging agent 1.

abundance of ^{19}F together with a large gyromagnetic ratio (i.e., 83% relative to ^1H) endows ^{19}F MRI with high sensitivity. The chemical shift range of ^{19}F MRI is over 400 ppm, which is about 20 times larger than that of conventional ^1H MRI. These features provide ^{19}F MRI with promising potential in various clinical applications, such as diagnosing disease,² evaluating therapy,³ tracking targets of interest,⁴ monitoring biochemical reactions,⁵ probing local pH or pO_2 ,⁶ and others. However, a high concentration of extraneous imaging agent is usually required for ^{19}F MRI because of the intrinsic low sensitivity of magnetic resonance. Therefore, it is of great importance to develop novel highly sensitive ^{19}F MRI agents.

Recently, we reported a dendrimer with 540 pseudosymmetrical fluorines as a highly sensitive ^{19}F MRI agent that demonstrated the strategy of using pseudosymmetry to improve the sensitivity of ^{19}F MRI.⁷ In this work, we applied this strategy to a novel ^{19}F MRI/fluorescence dual-modal imaging agent. Then, a star-shaped amphiphile **1** was designed as the target dual-modal imaging agent containing three parts: a fluorescent core (yellow), ^{19}F MRI signal emitters (green), and solubility enhancers (blue) (Figure 1). The fluorescent core is a planar highly conjugated system in which four substituted benzenes are connected to a central benzene through four acetylenes. To improve its ^{19}F MRI sensitivity, we introduced 48 symmetrical fluorines, which cumulatively give a single strong ^{19}F NMR signal, as ^{19}F MRI signal emitters. Eight monodisperse poly(ethylene glycol) (PEGs) are employed as biocompatible solubility enhancers. Overall, amphiphile **1** is considered to form unimolecular micelles in water with high aqueous solubility,⁸ high ^{19}F MRI sensitivity, and ^{19}F MRI/fluorescence dual functionality.

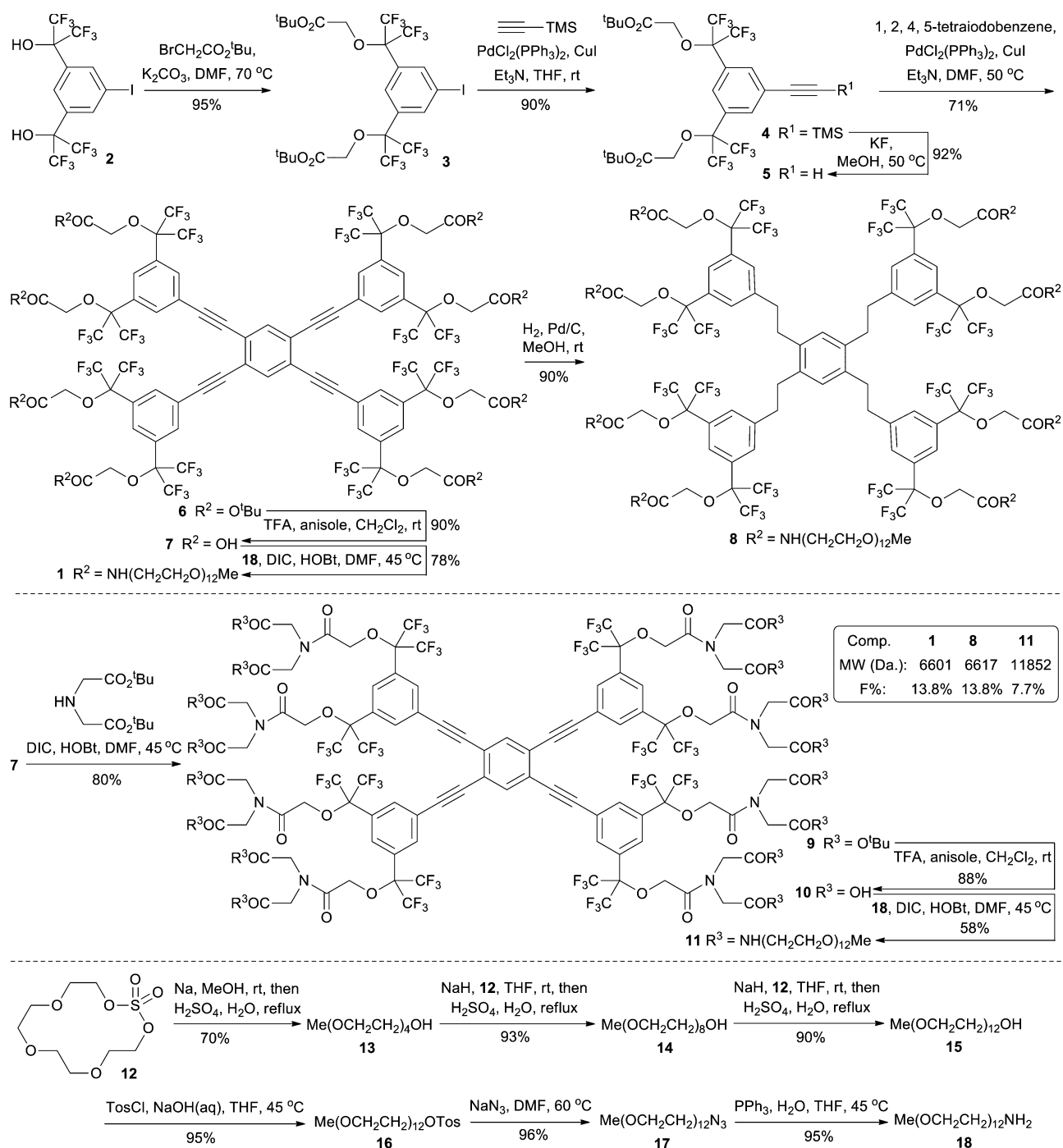
RESULTS AND DISCUSSION

A convergent synthesis of amphiphile **1** was carried out (Scheme 1). From iodobenzene **2**, the bis(trifluoromethyl)carbinols were reacted with *tert*-butyl bromoacetate in the presence of potassium carbonate to give *tert*-butyl ester **3**, which was then subjected Sonogashira coupling reaction with trimethylsilyl acetylene to provide trimethylsilyl phenylacetylene **4** in an 86% yield over two steps. After removal of the trimethylsilyl group in **4** with potassium fluoride, phenylacetylene **5** was coupled with 1,2,4,5-tetraiodobenzene at elevated temperature to give tetrasubstituted benzene **6** in a

65% yield over two steps. Removal of the *tert*-butyl groups in **6** with trifluoroacetic acid (TFA) in the presence of anisole provided octa acid **7** in a 90% yield. It is noteworthy that **7** was conveniently obtained by reverse extraction of impurities under basic conditions and precipitation of **7** at pH 3 from its aqueous solution. Octa acid **7** was then coupled with amine **18** in the presence of *N,N'*-diisopropylcarbodiimide (DIC) and 1-hydroxybenzotriazole (HOBt) to give target molecule **1** in a 78% yield. Monodisperse PEG-based amine **18** was prepared from macrocyclic sulfate **12** through an iterative nucleophilic ring-opening strategy developed in this group.⁹ Eventually, target molecule **1** was prepared on a 11-g scale in a 39% yield over six steps.

According to our previous study,¹⁰ amphiphile **1**, which has a fluorine content (13.8%) of less than 30% should have a high aqueous solubility. Indeed, **1** is freely soluble in water, and therefore, no formulation of **1** is required for downstream imaging and toxicity studies. An ^{19}F NMR study on an aqueous solution of amphiphile **1** was then carried out (Figure 2). As expected, **1** gave a sharp singlet ^{19}F NMR peak in deuterated chloroform from its 48 symmetrical fluorines. However, only a weak ^{19}F NMR signal was detected from its aqueous solution. Such a phenomenon is usually an indication of short relaxation times, which can “turn off” the ^{19}F NMR signal.¹¹ In fact, a short transverse relaxation time of **1** ($T_2 = 4.7$ ms; see Supporting Information, Figure S1) in water was found. There are a few reports on the self-assembly of amphiphilic conjugated π -molecules in water where π -stacking and hydrophobic interactions are the driving forces.¹² Therefore, the short T_2 of **1** is probably a result of its self-assembly into supermolecular structures. To “turn on” the ^{19}F NMR signal, it is necessary to tune the self-assembly by modifying the chemical structure of **1**. Therefore, two strategies were employed to tune the self-assembly: (1) breaking the molecular coplanarity by hydrogenation of the triple bonds in **1** to relieve the π -stacking and (2) increasing the hydrophilicity of **1** by introducing additional PEG units.

Accordingly, amphiphile **8** was then prepared by hydrogenation of **1** in the presence of palladium on carbon in a 90% yield (Scheme 1). Meanwhile, amphiphile **11** with eight additional pieces of monodisperse PEGs was prepared from **7**. After coupling of **7** with *tert*-butyl iminodiacetate, the *tert*-butyl protecting groups in ester **9** were removed with TFA to

Scheme 1. Synthesis of Amphiphiles **1**, **8**, and **11**

give hexadeca acid **10**, which was then coupled with **18**, providing **11** in a 41% yield over three steps (Scheme 1). As expected, both **8** and **11** gave strong ^{19}F NMR peaks (Figure 2) in both deuterated chloroform and water, and longer T_2 values for **8** and **11** were found (T_2 of **8**, 7.1 ms; T_2 of **11**, 15.8 ms; see Supporting Information, Figure S1). Therefore, the ^{19}F NMR signals were successfully turned on by tuning the self-assembly of the amphiphilic conjugated π -molecules through structural modifications.

To test the ^{19}F MRI sensitivities of these amphiphiles, ^{19}F MRI phantom experiments were then carried out on arrays of amphiphiles **1**, **8**, and **11** in water (Figure 3). The ^{19}F MRI phantom images showed dramatically different ^{19}F MRI-

detectable concentrations for these amphiphiles: 4.2 mM for **1**, 1.0 mM for **8**, and 0.5 mM for **11**. Compared to that of **1**, the ^{19}F MRI-detectable concentration of **11** was improved by a factor of 8.4. Recently, Resnati's group and our group reported highly sensitive ^{19}F MRI agents with the lowest detectable ^{19}F concentrations of 89 and 10 mM, respectively.^{8,13} Amphiphile **11** is detectable at an ^{19}F concentration of 24 mM with a scan time of 150 s. In terms of ^{19}F MRI sensitivity, **11** is one of the most sensitive ^{19}F MRI agents reported so far.

Based on the ^{19}F NMR and ^{19}F MRI observations, it is important to point out that the self-assembly pattern of a fluorinated amphiphile has a huge impact on the ^{19}F MRI sensitivity. Large self-assembled nanoparticles, which are usually

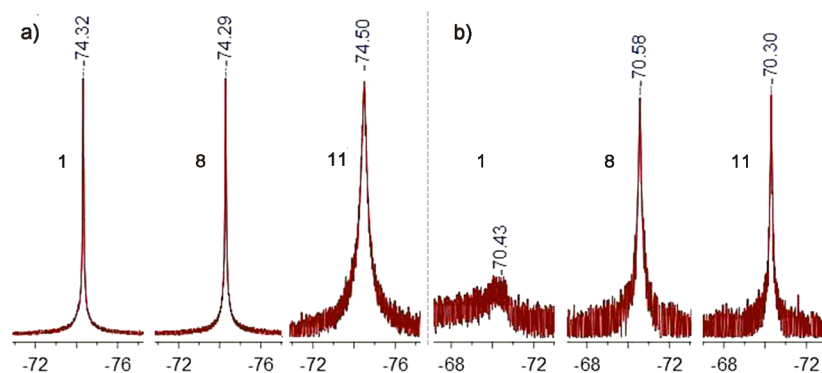


Figure 2. ^{19}F NMR spectra of amphiphiles **1**, **8**, and **11**: (a) 6.7 mM in CDCl_3 , (b) 6.7 mM in D_2O .

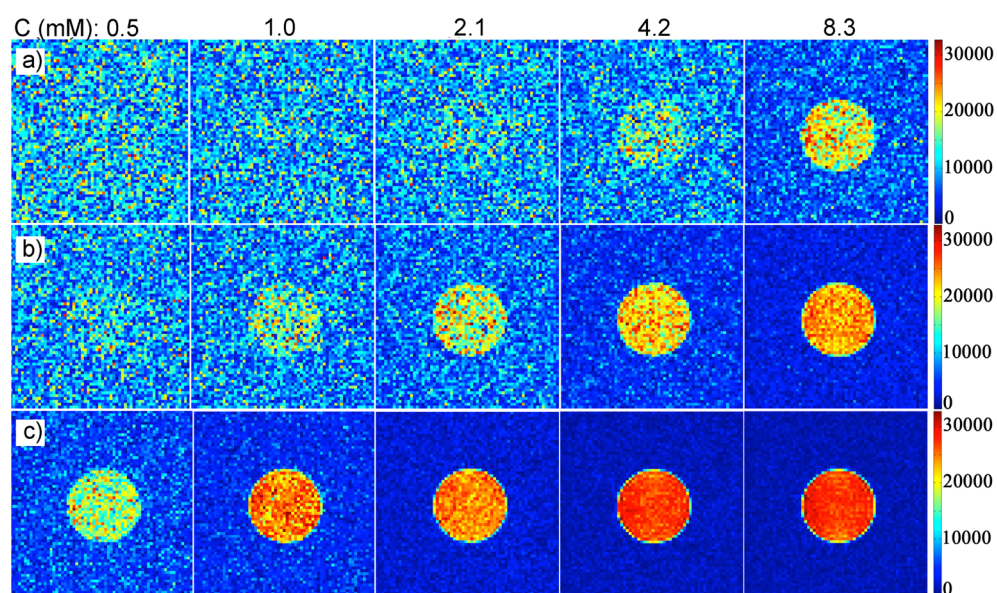


Figure 3. ^{19}F MRI phantom images of amphiphiles (a) **1**, (b) **8**, and (c) **11**.

accompanied by short T_2 , can turn off the ^{19}F NMR signal, whereas the ^{19}F NMR signal can be turned on by relieving the self-assembly or disassembling large nanoparticles through chemical or biological interference.^{11,14} In this case, we demonstrated that ^{19}F NMR signal can be turned on by tuning the particle size and shape by either breaking the coplanarity or improving the hydrophilicity. Therefore, it is crucial to take self-assembly into consideration during the design of novel amphiphilic ^{19}F MRI agents.

Next, the optical properties of these amphiphiles were investigated. First, the concentration-dependent UV spectra of these amphiphiles in water were collected (Figure 4a–c). All of the amphiphiles showed good concentration-dependent UV absorption. Amphiphile **1** has smooth UV absorption curves with a maximum absorption at 307 nm due to the formation of large supermolecular columns through π -stacking, which probably reduced the difference between energy levels in UV absorption. Meanwhile, **8** has much weaker absorption than **1** at short wavelength because the conjugated π -system in planar **1** was destroyed by hydrogenation of the four triple bonds to obtain **8**. Interestingly, **11** has more characterized UV absorption curves than **1**, which is an indication of weaker π -stacking in **11**. Second, the concentration-dependent fluorescence emission spectra of these amphiphiles were also collected (Figure 4d–f). Preferable concentration-dependent

fluorescence emissions were found in these amphiphiles. The fluorescence of **1** has two strong emission peaks at 393 and 445 nm as a result of the strong π -stacking. In contrast, **8** has a weak fluorescence emission peak at 376 nm. However, a strong fluorescence emission peak at 383 nm was observed for **11**. A blue fluorescent image of **11** in water was obtained under a routing UV lamp (see Supporting Information, Figure S2). Therefore, the combination of a high aqueous solubility, a high ^{19}F MRI sensitivity, and preferred fluorescence properties make **11** a promising ^{19}F MRI/fluorescence dual-imaging agent.

Finally, a toxicity study on ^{19}F MRI/fluorescence dual-imaging agent **11** was carried out. On one hand, **11** was incubated with HeLa cells in the concentration range of 0.1–100 μM . High cell viabilities at all concentrations of **11** indicated no observable toxicity. On the other hand, aqueous solutions of **11** were dosed to Kunming mice through tail vein injection. Again, no acute toxicity was observed even at a high dose of 10.0 g/kg. The mice were raised for 3 weeks until they were sacrificed for pathologic study. No pathology in internal organs was identified. Similar results were also obtained for amphiphiles **1** and **8**. Therefore, **11** is a highly biocompatible imaging agent without acute toxicity.

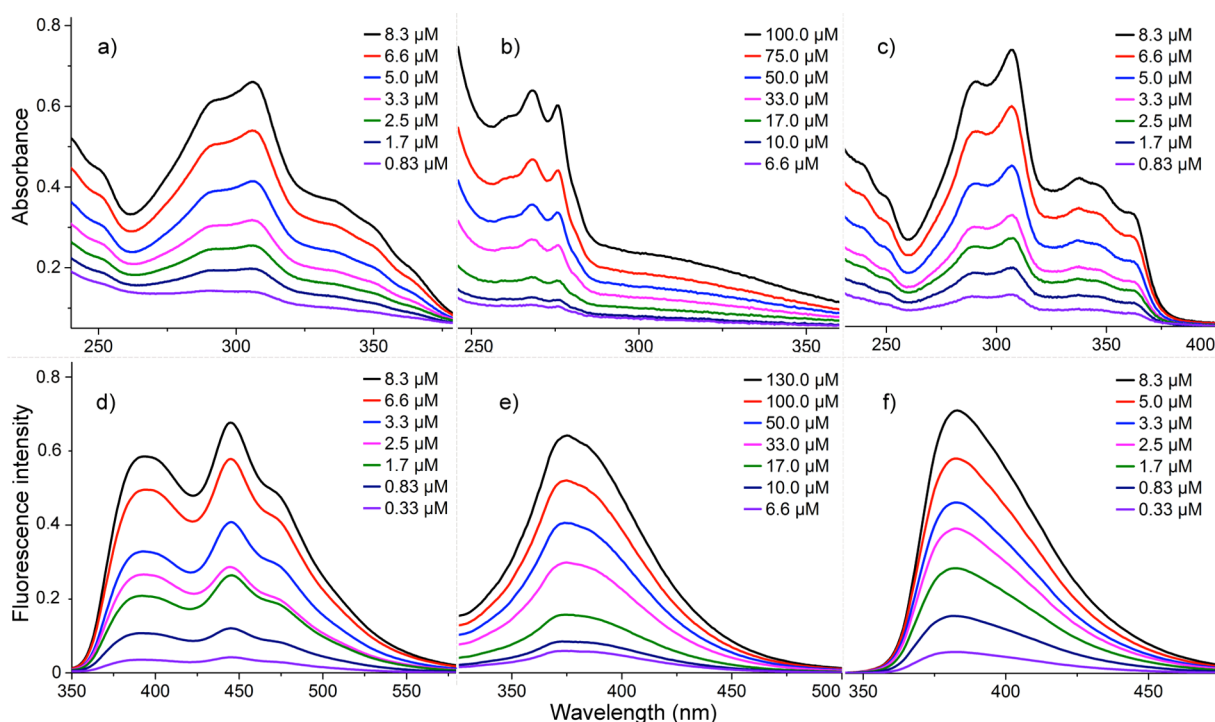


Figure 4. Concentration dependence of the (a–c) UV absorption and (d–f) fluorescence emission spectra of amphiphiles (a,d) **1**, (b,e) **8**, and (c,f) **11**.

CONCLUSIONS

In summary, a novel ^{19}F MRI/fluorescence dual-imaging agent with high aqueous solubility, high ^{19}F MRI sensitivity, and low toxicity has been successfully developed. Planar symmetry was successfully employed to incorporate 48 symmetrical fluorines with a single ^{19}F NMR signal and to simplify the synthesis. Such star-shaped fluorinated amphiphiles tend to self-assemble into supermolecular nanoparticles with distinctive ^{19}F NMR and fluorescence properties. It was found that hydrophobic interactions and π -stacking are driving forces for the self-assembly. Through tuning of coplanarity or hydrophilicity, the self-assembly of these amphiphiles can be monitored, and therefore, their ^{19}F NMR signals can be turned on or off. This study has thus laid a solid foundation for the design of smart nanodevices and ^{19}F MRI/fluorescence dual-imaging agents. In vivo studies with this ^{19}F MRI/fluorescence dual-imaging agent are currently in progress and will be published in due course.

EXPERIMENTAL SECTION

Bis-*tert*-butyl Ester 3. To a stirring mixture of alcohol **2** (32.2 g, 60.0 mmol) and K_2CO_3 (24.9 g, 180.0 mmol) in DMF (150 mL) was added *tert*-butyl bromoacetate (29.1 mL, 180.0 mmol) in one portion, and the resulting mixture was stirred at 70 °C for 3 h. Then, the mixture was diluted with ethyl acetate (EtOAc; 100 mL), filtered, washed with brine (300 mL, twice), and extracted with EtOAc (100 mL, three times). The combined organic layer was dried over anhydrous Na_2SO_4 , filtered, concentrated under a vacuum, and purified by column chromatography on silica gel (hexanes/EtOAc = 10/1) to give bis-*tert*-butyl ester **3** as a white wax (43.6 g, 95% yield). ^1H NMR (400 MHz, CDCl_3) δ 8.20 (s, 2H), 7.88 (s, 1H), 4.07 (s, 4H), 1.52 (s, 18H); ^{13}C NMR (100 MHz, CDCl_3) δ 166.1, 139.4, 130.9, 127.5, 121.9 (q, $J = 289.0$ Hz), 94.8, 83.2, 81.8–83.0 (m), 64.3, 28.1; ^{19}F NMR (376 MHz, CDCl_3) δ -74.09; MS (ESI) m/z 781.9 ($[\text{M} + \text{NH}_4]^+$; expected mass for $[\text{C}_{24}\text{H}_{29}\text{F}_{12}\text{INO}_6]^+$, 782.0); HRMS (ESI) calcd for $\text{C}_{24}\text{H}_{25}\text{F}_{12}\text{IO}_6\text{Na}$ ($[\text{M} + \text{Na}]^+$) 787.0396, found 787.0395.

Phenylacetylene 4. Under an atmosphere of argon, trimethylsilylacetylene (9.7 mL, 68.3 mmol) and Et_3N (50 mL) were sequentially added to a suspension of bis-*tert*-butyl ester **3** (43.5 g, 56.9 mmol), $\text{PdCl}_2(\text{PPh}_3)_2$ (0.4 g, 0.6 mmol), and CuI (0.2 g, 1.2 mmol) in THF (100 mL). The resulting mixture was stirred at room temperature for 8 h. After removal of the solvent under a vacuum, the residue was suspended in water (200 mL) and extracted with CH_2Cl_2 (150 mL, three times). The combined organic layer was dried over anhydrous Na_2SO_4 , filtered, concentrated under a vacuum, and purified by column chromatography on silica gel (hexanes/EtOAc = 10/1) to afford phenylacetylene **4** as a clear oil (37.6 g, 90% yield). ^1H NMR (400 MHz, CDCl_3) δ 7.92 (s, 2H), 7.84 (s, 1H), 4.06 (s, 4H), 1.52 (s, 18H), 0.26 (s, 9H); ^{13}C NMR (100 MHz, CDCl_3) δ 166.1, 133.7, 129.5, 127.8, 125.9, 122.0 (q, $J = 289.0$ Hz), 102.4, 97.8, 83.0, 82.2–82.8 (m), 64.3, 28.0, -0.4; ^{19}F NMR (376 MHz, CDCl_3) δ -74.06; MS (ESI) m/z 757.1 ($[\text{M} + \text{Na}]^+$; expected mass for $[\text{C}_{29}\text{H}_{34}\text{F}_{12}\text{O}_6\text{SiNa}]^+$, 757.2), 773.1 ($[\text{M} + \text{K}]^+$; expected mass for $[\text{C}_{29}\text{H}_{34}\text{F}_{12}\text{O}_6\text{SiK}]^+$, 773.2); HRMS (ESI) calcd for $\text{C}_{29}\text{H}_{34}\text{F}_{12}\text{O}_6\text{SiNa}$ ($[\text{M} + \text{Na}]^+$) 757.1825, found 757.1848.

Tetra-*tert*-butyl Ester 5. To a solution of phenylacetylene **4** (37.5 g, 51.0 mmol) in methanol (150 mL) was added KF (5.9 g, 102.0 mmol) in one portion. The reaction mixture was then heated to 50 °C and stirred at this temperature for 1 h. After removal of the methanol under a vacuum, the residue was purified by column chromatography on silica gel (hexanes/EtOAc = 10/1) to give *tert*-butyl ester **5** as a white wax (31.1 g, 92% yield). ^1H NMR (400 MHz, CDCl_3) δ 7.96 (s, 2H), 7.89 (s, 1H), 4.06 (s, 4H), 3.21 (s, 1H), 1.51 (s, 18H); ^{13}C NMR (100 MHz, CDCl_3) δ 166.1, 134.0, 129.7, 128.2, 124.8, 122.0 (q, $J = 288.0$ Hz), 83.1, 82.4–83.0 (m), 81.4, 80.2, 64.4, 28.0; ^{19}F NMR (376 MHz, CDCl_3) δ -74.17; MS (ESI) m/z 701.1 ($[\text{M} + \text{K}]^+$; expected mass for $[\text{C}_{26}\text{H}_{26}\text{F}_{12}\text{O}_6\text{K}]^+$, 701.1); HRMS (ESI) calcd for $\text{C}_{26}\text{H}_{26}\text{F}_{12}\text{O}_6\text{Na}$ ($[\text{M} + \text{Na}]^+$) 685.1430, found 685.1458.

Tetrasubstituted Benzene 6. Under an atmosphere of argon, *tert*-butyl ester **5** (31.0 g, 46.8 mmol) was added to a stirring suspension of 1,2,4,5-tetraiodobenzene (4.5 g, 7.8 mmol), $\text{Pd}(\text{PPh}_3)_2\text{Cl}_2$ (0.6 g, 0.8 mmol), and CuI (0.2 g, 1.6 mmol) in degassed DMF (100 mL) and Et_3N (50 mL). Then, the reaction mixture was heated to 50 °C and stirred at this temperature for 24 h. The reaction mixture was suspended in water (300 mL) and extracted with CH_2Cl_2

(150 mL, three times). The combined organic layer was dried over anhydrous Na_2SO_4 , filtered, concentrated under a vacuum, and purified by column chromatography on silica gel (hexanes/EtOAc = 5/1) to give tetrasubstituted benzene **6** as a yellow wax (15.1 g, 71% yield). ^1H NMR (400 MHz, CDCl_3) δ 7.99 (s, 8H), 7.97 (s, 4H), 7.83 (s, 2H), 4.07 (s, 16H), 1.49 (s, 72H); ^{13}C NMR (100 MHz, CDCl_3) δ 166.0, 136.0, 133.4, 130.0, 128.4, 125.3, 124.8, 121.9 (q, $J = 288.0$ Hz), 93.6, 88.8, 83.0, 82.0–82.9 (m), 64.3, 28.0; ^{19}F NMR (376 MHz, CDCl_3) δ -74.25; HRMS (ESI) calcd for $\text{C}_{110}\text{H}_{106}\text{F}_{48}\text{NO}_{24}$ ($[\text{M} + \text{NH}_4]^+$) 2737.6372, found 2737.6361.

Octa Acid 7. To a stirring solution of tetrasubstituted benzene **6** (15.0 g, 5.5 mmol) and anisole (7.1 mL, 66.0 mmol) in CH_2Cl_2 (100 mL) was added trifluoroacetic acid (33.5 mL, 440.0 mmol). The reaction mixture was stirred at room temperature for 4 h and then concentrated under a vacuum. The residue was dissolved in NaOH (1 N, 40 mL) and extracted with CH_2Cl_2 (20 mL, twice). The aqueous layer was acidified by hydrochloric acid (1 N, 45 mL) to pH 3, and the precipitate was collected and dried under a vacuum to afford octa acid **7** as a yellow wax (11.2 g, 90% yield). ^1H NMR (400 MHz, CDCl_3) δ 8.15 (s, 8H), 8.11 (s, 4H), 8.04 (s, 2H), 4.34 (s, 16H); ^{19}F NMR (376 MHz, CDCl_3) δ -71.97; MS (ESI) m/z 2270.7 ($[\text{M} + \text{H}]^+$); expected mass for $[\text{C}_{78}\text{H}_{39}\text{F}_{48}\text{O}_{24}]^+$, 2271.1; HRMS (ESI) calcd for $\text{C}_{78}\text{H}_{38}\text{F}_{48}\text{O}_{24}\text{Na}$ ($[\text{M} + \text{Na}]^+$) 2293.0884, found 2293.0845.

Amphiphile 1. Under an atmosphere of argon, DIC (4.0 mL, 26.4 mmol) was added to a stirring solution of HOBT (3.6 g, 26.4 mmol) and octa acid **7** (5.0 g, 2.2 mmol) in DMF (100 mL) at 0 °C. After 20 min, amine **18** (14.8 g, 26.4 mmol) was added in one portion at room temperature, and the reaction mixture was stirred at 45 °C for 12 h. The reaction mixture was washed with brine (200 mL) and extracted with CH_2Cl_2 (150 mL, four times). The combined organic layer was dried over anhydrous Na_2SO_4 , concentrated under a vacuum, and purified by column chromatography on silica gel [CH_2Cl_2 /methanol (MeOH) = 10/1] to give amphiphile **1** as a yellow oil (11.3 g, 78% yield). ^1H NMR (400 MHz, CDCl_3) δ 7.97 (s, 2H), 7.93 (s, 4H), 7.82 (s, 8H), 4.03 (s, 16H), 3.63–3.66 (m, 352H), 3.54–3.56 (m, 32H), 3.38 (s, 24H); ^{13}C NMR (100 MHz, CDCl_3) δ 165.6, 132.8, 128.8, 127.4, 124.7, 124.6, 121.2 (q, $J = 288.0$ Hz), 92.9, 88.7, 81.5–82.6 (m), 71.4, 70.1, 70.0, 69.8, 69.0, 65.1, 58.4, 38.9, 29.1; ^{19}F NMR (376 MHz, CDCl_3) δ -74.24; MS (MALDI-TOF) m/z 6627.9 ($[\text{M} + \text{HCN}]^+$); expected mass for $[\text{C}_{279}\text{H}_{447}\text{F}_{48}\text{N}_9\text{O}_{12}]^+$, 6627.9.

Amphiphile 8. A suspension of amphiphile **1** (6.6 g, 1.0 mmol) and palladium on carbon (0.7 g, 10 wt %) in methanol (50 mL) was stirred under an atmosphere of hydrogen (4.0 MPa) at room temperature for 12 h. Then, the mixture was filtered and concentrated under a vacuum. The residue was purified by column chromatography on silica gel (CH_2Cl_2 /MeOH = 10/1) to give amphiphile **8** as a white oil (6.0 g, 90% yield). ^1H NMR (400 MHz, CDCl_3) δ 7.64 (s, 2H), 7.44 (s, 8H), 7.38 (s, 4H), 3.98 (s, 16H), 3.64–3.66 (m, 352H), 3.54–3.57 (m, 32H), 3.38 (s, 24H), 2.94 (s, 8H), 2.94 (s, 8H); ^{13}C NMR (100 MHz, CDCl_3) δ 165.6, 143.4, 135.5, 129.9, 127.5, 125.4, 121.1 (q, $J = 288.0$ Hz), 81.5–82.5 (m), 71.2, 69.8, 69.6, 69.0, 64.9, 58.2, 38.6, 36.4, 32.6, 27.2; ^{19}F NMR (376 MHz, CDCl_3) δ -74.27; MS (MALDI-TOF) m/z 6640.4 ($[\text{M} + \text{Na}]^+$); expected mass for $[\text{C}_{278}\text{H}_{462}\text{F}_{48}\text{N}_{24}\text{O}_{112}\text{Na}]^+$, 6640.0.

Hexadeca-tert-butyl Ester 9. Under an atmosphere of argon, DIC (4.9 mL, 31.7 mmol) was added to a stirring solution of HOBT (4.3 g, 31.7 mmol) and octa acid **7** (6.0 g, 2.6 mmol) in DMF (100 mL) at 0 °C. After 20 min, di-tert-butyl 2,2'-azanediyl diacetate (7.8 g, 31.7 mmol) was added, and the mixture was stirred at 45 °C for an additional 12 h. The reaction mixture was washed with brine (200 mL) and extracted with CH_2Cl_2 (100 mL, three times). The combined organic layer was dried over anhydrous Na_2SO_4 , filtered, concentrated under a vacuum, and purified by column chromatography (hexanes/EtOAc = 4/1) to give hexadeca-tert-butyl ester **9** as a yellowish wax (8.8 g, 80% yield). ^1H NMR (400 MHz, CDCl_3) δ 7.97 (s, 4H), 7.93 (s, 10H), 4.30 (s, 16H), 4.07 (d, $J = 8.0$ Hz, 32H), 1.43 (d, $J = 8.0$ Hz, 144H); ^{13}C NMR (100 MHz, CDCl_3) δ 167.6, 166.4, 133.4, 129.5, 128.2, 125.1, 121.8 (q, $J = 288.0$ Hz), 93.3, 89.1, 82.9, 82.1, 65.4, 49.1, 28.0 (d, $J = 150.0$ Hz); ^{19}F NMR (376 MHz, CDCl_3) δ -73.94; MS

(MALDI-TOF) m/z 4088.7 ($[\text{M} + \text{H}]^+$); expected mass for $[\text{C}_{174}\text{H}_{207}\text{F}_{48}\text{N}_8\text{O}_{48}]^+$, 4088.3.

Hexadeca Acid 10. Hexadeca acid **10** was prepared from hexadeca-tert-butyl ester **9** by following the same procedure as used for the preparation of octa acid **7** and was obtained as a yellowish wax in an 88% yield. ^1H NMR (400 MHz, CDCl_3) δ 8.14 (s, 8H), 8.12 (s, 4H), 8.08 (s, 2H), 4.55 (s, 16H), 4.32 (s, 16H), 4.26 (s, 16H); ^{19}F NMR (376 MHz, CDCl_3) δ -71.75; MS (MALDI-TOF) m/z 3212.2 ($[\text{M} + \text{Na}]^+$); expected mass for $[\text{C}_{110}\text{H}_{77}\text{F}_{48}\text{N}_8\text{O}_{48}\text{Na}]^+$, 3212.3.

Amphiphile 11. Amphiphile **11** was prepared from hexadeca acid **10** by following the same procedure as used for the preparation of amphiphile **1** and was obtained as a yellowish oil in a 58% yield. ^1H NMR (400 MHz, CDCl_3) δ 7.98 (s, 8H), 7.78 (s, 2H), 7.65 (s, 4H), 4.13 (s, 16H), 3.85 (s, 32H), 3.29–3.47 (m, 778H), 3.20 (s, 48H); ^{13}C NMR (100 MHz, CDCl_3) δ 168.8, 168.2, 166.6, 132.5, 128.9, 124.2, 121.7 (q, $J = 290.0$ Hz), 81.7–82.8 (m), 71.3, 69.9, 69.8, 69.6, 68.9, 68.5, 64.6, 58.3, 52.7, 38.8, 29.0; ^{19}F NMR (376 MHz, CDCl_3) δ -74.49; MS (MALDI-TOF) m/z 11868.2 ($[\text{M} + \text{NH}_3]^+$); expected mass for $[\text{C}_{510}\text{H}_{897}\text{F}_{48}\text{N}_{25}\text{O}_{224}]^+$, 11868.9.

Monomethylated PEG₄ 13. Under an atmosphere of argon, sodium (5.5 g, 240.0 mmol) was slowly added to anhydrous MeOH (100 mL), and the mixture was refluxed for 30 min. Then, a solution of macrocyclic sulfate **12** (41.0 g, 160.0 mmol) in anhydrous MeOH (40 mL) was slowly added, and the mixture was stirred at room temperature for 12 h. Then, water (4.3 mL, 240.0 mmol) and H_2SO_4 (6.5 mL, 120.0 mmol) were added, and the resulting mixture was refluxed for 1 h. The reaction was quenched with saturated NaHCO_3 solution (200 mL), and MeOH was removed under a vacuum. The residue was extracted with CH_2Cl_2 (100 mL, three times). The combined organic layer was dried over anhydrous Na_2SO_4 , concentrated under a vacuum, and purified by column chromatography on silica gel (CH_2Cl_2 /MeOH = 20/1) to give monomethylated PEG₄ **13** as a clear oil (23.3 g, 70% yield). ^1H NMR (400 MHz, CDCl_3) δ 3.71–3.73 (m, 2H), 3.64–3.67 (m, 10H), 3.61–3.63 (m, 2H), 3.56–3.57 (m, 2H), 3.38 (s, 3H), 3.17 (s, 1H).

Monomethylated PEG₈ 14. Under an atmosphere of argon, a solution of monomethylated PEG₄ **13** (23.0 g, 110.5 mmol) in THF (50 mL) was added dropwise into a suspension of NaH (4.0 g, 165.8 mmol) in THF (100 mL) at room temperature. After this mixture had been stirred for an additional 30 min, a solution of macrocyclic sulfate **12** (42.5 g, 165.8 mmol) in THF (50 mL) was added, and the resulting mixture was stirred at room temperature for an additional 12 h. Then, water (3.0 mL, 165.8 mmol) and H_2SO_4 (4.5 mL, 82.9 mmol) were added, and the resulting mixture was refluxed for 1 h. The mixture was neutralized with saturated NaHCO_3 solution (200 mL) and extracted with CH_2Cl_2 (150 mL, four times). The combined organic layer was dried over anhydrous Na_2SO_4 , concentrated under a vacuum, and purified by column chromatography on silica gel (CH_2Cl_2 /MeOH = 20/1) to give monomethylated PEG₈ **14** as a clear oil (39.5 g, 93% yield). ^1H NMR (400 MHz, CDCl_3) δ 3.71–3.73 (m, 2H), 3.64–3.67 (m, 26H), 3.59–3.62 (m, 2H), 3.54–3.56 (m, 2H), 3.38 (s, 3H), 3.03 (s, 1H).

Monomethylated PEG₁₂ 15. Monomethylated PEG₁₂ **15** was prepared from monomethylated PEG₈ **14** by following the same procedure as used for the preparation of monomethylated PEG₈ **14** and was obtained as a clear oil in a 90% yield. ^1H NMR (400 MHz, CDCl_3) δ 3.71–3.73 (m, 4H), 3.63–3.67 (m, 40H), 3.59–3.62 (m, 2H), 3.54–3.56 (m, 2H), 3.38 (s, 3H), 2.80 (s, 1H).

Methylbenzenesulfonate 16. A solution of *p*-toluenesulfonyl chloride (34.7 g, 182.0 mmol) in THF (50 mL) was slowly added to a stirring solution of monomethylated PEG₁₂ **15** (51.0 g, 91.0 mmol) and NaOH (8.8 N, 30 mL) in THF (150 mL) at 0 °C over 1 h, and the resulting mixture was stirred at 45 °C for 4 h. Then, the reaction mixture was diluted with brine (200 mL) and extracted with CH_2Cl_2 (150 mL, three times). The combined organic layer was dried over anhydrous Na_2SO_4 , concentrated under a vacuum, and purified by column chromatography on silica gel (CH_2Cl_2 /MeOH = 20/1) to give methylbenzenesulfonate **16** as a clear oil (61.8 g, 95% yield). ^1H NMR (400 MHz, CDCl_3) δ 7.71 (d, $J = 8.0$ Hz, 2H), 7.24 (d, $J = 8.0$ Hz,

2H), 4.06–4.09 (m, 2H), 3.54–3.56 (m, 46H), 3.29 (s, 3H), 2.39 (s, 3H).

Azido 17. To a solution of methylbenzenesulfonate **16** (61.0 g, 85.4 mmol) in DMF (150 mL) was added NaN₃ (11.1 g, 170.8 mmol), and the reaction mixture was stirred at 60 °C for 3 h. The reaction mixture was diluted with brine (200 mL) and extracted with CH₂Cl₂ (150 mL, three times). The combined organic layer was dried over anhydrous Na₂SO₄, filtered, concentrated under a vacuum, and purified by column chromatography on silica gel (CH₂Cl₂/MeOH = 20/1) to give azido **17** as a clear oil (48.0 g, 96% yield). ¹H NMR (400 MHz, CDCl₃) δ 3.63–3.69 (m, 46H), 3.54–3.56 (m, 2H), 3.37 (s, 3H); ¹³C NMR (100 MHz, CDCl₃) δ 71.7, 70.5, 70.4, 69.9, 58.8, 50.5; HRMS (ESI) calcd for C₂₅H₅₂NO₁₂ ([M + H–N₂]⁺) 558.3484, found 558.3473.

Amine 18. At room temperature, triphenyl phosphine (31.8 g, 121.2 mmol) was added to a solution of azido **17** (47.5 g, 81.1 mmol) in THF (100 mL), and the mixture was stirred at 45 °C for 4 h. Then, water (7.3 mL, 405.5 mmol) was added, and the reaction mixture was stirred at 45 °C for an additional 4 h. The reaction mixture was concentrated under a vacuum and purified by column chromatography on silica gel (CH₂Cl₂/MeOH = 20/1) to afford amine **18** as a clear oil (43.1 g, 95% yield). ¹H NMR (400 MHz, CDCl₃) δ 3.65–3.66 (m, 44H), 3.54–3.57 (m, 4H), 3.38 (s, 3H), 2.44 (s, 2H); ¹³C NMR (100 MHz, CDCl₃) δ 71.6, 70.2, 69.8, 68.9, 58.7, 39.8; HRMS (ESI) calcd for C₂₅H₅₄NO₁₂ ([M + H]⁺) 560.3641, found 560.3638.

■ ASSOCIATED CONTENT

■ Supporting Information

Relaxation times; fluorescence images of amphiphiles; and copies of ¹H, ¹⁹F, and ¹³C NMR, and HRMS spectra of compounds. The Supporting Information is available free of charge on the ACS Publications website at DOI: 10.1021/acs.joc.5b00810.

■ AUTHOR INFORMATION

Corresponding Authors

*E-mail: zhengxing5018@yahoo.com (X.Z.).

*E-mail: zxjiang@whu.edu.cn (Z.-X.J.).

Notes

The authors declare no competing financial interest.

■ ACKNOWLEDGMENTS

This work was financially supported by the National Natural Science Foundation of China (21372181, 81227902, 21305156, and 81273537).

■ REFERENCES

- (1) For recent reviews, see: (a) Lee, J. E.; Lee, N.; Kim, T.; Kim, J.; Hyeon, T. *Acc. Chem. Res.* **2011**, *44*, 893–902. (b) Lee, D.-E.; Koo, H.; Sun, I.-C.; Ryu, J. H.; Kim, K.; Kwon, I. C. *Chem. Soc. Rev.* **2012**, *41*, 2656–2672. (c) Jin, Y. *Acc. Chem. Res.* **2014**, *47*, 138–148.
- (2) (a) Yanagisawa, D.; Amatsubo, T.; Morikawa, S.; Taguchi, H.; Urushitani, M.; Shirai, N.; Hirao, K.; Shiino, A.; Inubushi, T.; Tooyama, I. *Neuroscience* **2011**, *184*, 120–127. (b) Chen, S.; Yang, Y.; Li, H.; Zhou, X.; Liu, M. *Chem. Commun.* **2014**, *50*, 283–285.
- (3) Halaweish, A. F.; Moon, R. E.; Foster, W. M.; Soher, B. J.; McAdams, H. P.; MacFall, J. R.; Ainslie, M. D.; MacIntyre, N. R.; Charles, H. C. *Chest* **2013**, *144*, 1300–1310.
- (4) (a) Ahrens, E. T.; Flores, R.; Xu, H.; Morel, P. A. *Nat. Biotechnol.* **2005**, *23*, 983–987. (b) Janjic, J. M.; Srinivas, M.; Kadayakkara, D. K.; Ahrens, E. T. *J. Am. Chem. Soc.* **2008**, *130*, 2832–2841.
- (5) (a) Mizukami, S.; Takikawa, R.; Sugihara, F.; Hori, Y.; Tochio, H.; Walchli, M.; Shirakawa, M.; Kikuchi, K. *J. Am. Chem. Soc.* **2008**, *130*, 794–795. (b) Mizukami, S.; Takikawa, R.; Sugihara, F.; Shirakawa, M.; Kikuchi, K. *Angew. Chem., Int. Ed.* **2009**, *48*, 3641–3643.

(6) (a) Takaoka, Y.; Kiminami, K.; Mizusawa, K.; Matsuo, K.; Narazaki, M.; Matsuda, T.; Hamachi, I. *J. Am. Chem. Soc.* **2011**, *133*, 11725–11731. (b) Goswami, L. N.; Khan, A. A.; Jalisatgi, S. S.; Hawthorne, M. F. *Chem. Commun.* **2014**, *50*, 5793–5795.

(7) Yu, W.; Yang, Y.; Bo, S.; Li, Y.; Chen, S.; Yang, Z.; Zheng, X.; Jiang, Z.-X.; Zhou, X. *J. Org. Chem.* **2015**, *80*, 4443–4449.

(8) Taraban, M. B.; Li, Y.; Yue, F.; Jouravleva, E. V.; Anisimov, M. A.; Jiang, Z.-X.; Yu, Y. B. *RSC Adv.* **2014**, *4*, 54565–54575.

(9) Zhang, H.; Li, X.; Shi, Q.; Li, Y.; Xia, G.; Chen, L.; Yang, Z.; Jiang, Z.-X. *Angew. Chem., Int. Ed.* **2015**, *54*, 3763–3767.

(10) (a) Li, Y.; Thapa, B.; Zhang, H.; Li, X.; Yu, F.; Jeong, E.-K.; Yang, Z.; Jiang, Z.-X. *Tetrahedron* **2013**, *69*, 9586–9590. (b) Li, Y.; Guo, Q.; Li, X.; Zhang, H.; Yu, F.; Yu, W.; Xia, G.; Fu, M.; Yang, Z.; Jiang, Z.-X. *Tetrahedron Lett.* **2014**, *55*, 2110–2113.

(11) (a) Mizukami, S.; Takikawa, R.; Sugihara, F.; Hori, Y.; Tochio, H.; Walchli, M.; Shirakawa, M.; Kikuchi, K. *J. Am. Chem. Soc.* **2008**, *130*, 794–795. (b) Takaoka, Y.; Sakamoto, T.; Tsukiji, S.; Narazaki, M.; Matsuda, T.; Tochio, H.; Shirakawa, M.; Hamachi, I. *Nat. Chem.* **2009**, *1*, 557–561.

(12) (a) Percec, V.; Glodde, M.; Bera, T. K.; Miura, Y.; Shiyonovskaya, I.; Singer, K. D.; Balagurusamy, V. S. K.; Heiney, P. A.; Schnell, I.; Rapp, A.; Spiess, H.-W.; Hudson, S. D.; Duan, H. *Nature* **2002**, *419*, 384–387. (b) Wu, J.; Li, J.; Kolb, U.; Müllen, K. *Chem. Commun.* **2006**, *42*, 48–50. (c) Zhang, S.; Sun, H.-J.; Hughes, A. D.; Moussodia, R.-O.; Bertin, A.; Chen, Y.; Pochan, D. J.; Heiney, P. A.; Klein, M. L.; Percec, V. *Proc. Natl. Acad. Sci. U.S.A.* **2014**, *111*, 9058–9063.

(13) Tirota, I.; Mastropietro, A.; Cordiglieri, C.; Gazzera, L.; Baggi, F.; Baselli, G.; Bruzzone, M. G.; Zucca, I.; Cavallo, G.; Terraneo, G.; Bombelli, F. B.; Metrangolo, P.; Resnati, G. *J. Am. Chem. Soc.* **2014**, *136*, 8524–8527.

(14) Yuan, Y.; Sun, H.; Ge, S.; Wang, M.; Zhao, H.; Wang, L.; An, L.; Zhang, J.; Zhang, H.; Hu, B.; Wang, J.; Liang, G. *ACS Nano* **2015**, *9*, 761–768.

(15) Zhong, K.-L.; Wang, Z.; Liang, Y.; Chen, T.; Yin, B.; Jin, Y. *Supramol. Chem.* **2014**, *26*, 729–735.